α-attractors in quintessential inflation motivated by supergravity

L. Aresté Saló[1,*] D. Benisty[2,3,4,†] E. I. Guendelman[2,3,5,‡] and J. d. Haro[6,§]

[1]*School of Mathematical Sciences, Queen Mary University of London,*
Mile End Road, London E1 4NS, United Kingdom
[2]*Physics Department, Ben-Gurion University of the Negev, Beer-Sheva 84105, Israel*
[3]*Frankfurt Institute for Advanced Studies (FIAS), Ruth-Moufang-Strasse 1,*
60438 Frankfurt am Main, Germany
[4]*DAMTP, Centre for Mathematical Sciences, University of Cambridge,*
Wilberforce Road, Cambridge CB3 0WA, United Kingdom
[5]*Bahamas Advanced Study Institute and Conferences, 4A Ocean Heights,*
Hill View Circle, Stella Maris, Long Island, The Bahamas
[6]*Departament de Matemàtiques, Universitat Politècnica de Catalunya,*
Diagonal 647, 08028 Barcelona, Spain

An exponential kind of quintessential inflation potential motivated by supergravity is studied. This type belongs to the class of α-attractor models. The model was studied for the first time by Dimopoulos and Owen in [J. Cosmol. Astropart. Phys. 06 (2017) 027], in which the authors introduced a negative cosmological constant in order to ensure a zero-vacuum energy density at late times. However, in this paper, we disregard this cosmological constant, showing that the obtained results are very close to the ones obtained recently in the context of Lorentzian quintessential inflation and thus depicting with great accuracy the early- and late-time acceleration of our Universe. The model is compatible with the recent observations. Finally, we review the treatment of the α-attractor and we show that our potential depicts the late time cosmic acceleration with an effective equation of state equal to −1.

I. INTRODUCTION

The inflationary paradigm is considered as a necessary part of the standard model of cosmology, since it provides the solution to the horizon, the flatness, and the monopole problems [1–9]. It can be achieved through various mechanisms, for instance, through the introduction of a scalar inflaton field [10–34]. The well-known Starobinsky model [35] (see also Ref. [36] for a review), originally conceived to find nonsingular solutions going beyond general relativity—although it really only contains one unstable nonsingular solution—is one of the best candidates to correctly depict the inflationary period, in the sense that the theoretical results provided by the model match perfectly with the current observation data [37–39]. An important extension of the Starobinsky model, coming from supergravity, are the so-called α-attractors [40–48], which also depict inflation very well and are used for the first time in the context of quintessential inflation—see the papers [49–58] for a detailed explanation of the early and recent results of

this topic—in Ref. [59] (see also Ref. [60]). In that paper, the authors also introduce a negative cosmological constant (CC) in order to have at late times an exponential potential which guarantees an eternal acceleration for a wide range of the parameters involved in the model or getting a transient acceleration at the present time.

However, as we will show in this paper, for this simple model, which only depends on two parameters, quintessential inflation is also obtained without the introduction of this CC. In fact, the model leads to the same results provided by Lorentzian quintessential inflation [61–63]; i.e., the model behaves as an α-attractor at early times and provides, at late times, an eternal inflation with an effective equation of state (EoS) parameter equal to −1 at very late times.

The paper is organized as follows. In Sec. II, we calculate the power spectrum of perturbations and the value of the parameters involved in the model in agreement with the observational data at early and late times. Section III is devoted to the analytic calculation of the value of the field and its derivative at the reheating time, which is needed to perform the numerical calculations up to the present and future times. In Sec. IV, we perform the numerical calculations, showing that at late times the Universe enters in an eternal acceleration and, at the present time, the

*[*]l.arestesalo@qmul.ac.uk
[†]benidav@post.bgu.ac.il
[‡]guendel@bgu.ac.il
[§]jaime.haro@upc.edu

effective EoS parameter, given by the model, agrees with the Planck's results. Section VI introduces a CC, and there we review the work done in Ref. [59], showing that the model with a CC is only compatible with Planck's observational data for a narrow range of values of the parameter α, which, from our point of view, does not prove its viability.

The units used throughout the paper are $\hbar = c = 1$, and we denote the reduced Planck mass by $M_{pl} \equiv \frac{1}{\sqrt{8\pi G}} \cong 2.44 \times 10^{18}$ GeV.

II. α-ATTRACTORS IN QUINTESSENTIAL INFLATION

We consider the following Lagrangian motivated by supergravity and corresponding to a nontrivial Kähler manifold (see, for instance, Ref. [59] and the references therein), combined with an standard exponential potential,

$$\mathcal{L} = \frac{1}{2} \frac{\dot{\phi}^2}{(1 - \frac{\phi^2}{6\alpha})^2} M_{pl}^2 - \lambda M_{pl}^4 e^{-\kappa\phi}, \qquad (1)$$

where ϕ is a dimensionless scalar field and κ and λ are positive dimensionless constants.

For the kinetic term to have the canonical form, one can redefine the scalar field as

$$\phi = \sqrt{6\alpha} \tanh\left(\frac{\varphi}{\sqrt{6\alpha}M_{pl}}\right), \qquad (2)$$

obtaining the potential

$$V(\varphi) = \lambda M_{pl}^4 e^{-n \tanh\left(\frac{\varphi}{\sqrt{6\alpha}M_{pl}}\right)}, \qquad (3)$$

where we have introduced the dimensionless parameter $n = \kappa\sqrt{6\alpha}$. Similarly to Refs. [61–63], the potential satisfies the *cosmological seesaw mechanism*, where the left side of the potential gives a very large energy density—the inflationary side–and the right side gives a very small energy density—the dark energy side. The asymptotic values are $V_{\pm} = \lambda \exp(\pm n)$. The parameter n is the logarithm of the ratios between the energy densities, as ξ in the earlier versions [63]. Dealing with this potential at early times, the slow-roll parameters are given by

$$\epsilon \equiv \frac{M_{pl}^2}{2} \left(\frac{V_\varphi}{V}\right)^2 = \frac{n^2}{12\alpha} \frac{1}{\cosh^4(\frac{\varphi}{\sqrt{6\alpha}M_{pl}})}, \qquad (4)$$

where we must assume that $\frac{n^2}{12\alpha} > 1$ because inflation ends when $\epsilon_{END} = 1$, and the other slow-roll parameter is

$$\eta \equiv M_{pl}^2 \frac{V_{\varphi\varphi}}{V} = \frac{n}{3\alpha} \left[\frac{\tanh\left(\frac{\varphi/M_{pl}}{\sqrt{6\alpha}}\right)}{\cosh^2\left(\frac{\varphi/M_{pl}}{\sqrt{6\alpha}}\right)} + \frac{n/2}{\cosh^4\left(\frac{\varphi/M_{pl}}{\sqrt{6\alpha}}\right)} \right]. \qquad (5)$$

Both slow-roll parameters have to be evaluated when the pivot scale leaves the Hubble radius, which will happen for large values of $\cosh(\frac{\varphi}{\sqrt{6\alpha}M_{pl}})$, obtaining

$$\epsilon_* = \frac{n^2}{12\alpha} \frac{1}{\cosh^4\left(\frac{\varphi_*/M_{pl}}{\sqrt{6\alpha}}\right)}, \qquad \eta_* \cong -\frac{n}{3\alpha} \frac{1}{\cosh^2\left(\frac{\varphi_*/M_{pl}}{\sqrt{6\alpha}}\right)}, \qquad (6)$$

with $\varphi_* < 0$.

Next, we calculate the number of e-folds from the leaving of the pivot scale to the end of inflation, which for small values of α is given by

$$N = \frac{1}{M_{pl}} \int_{\varphi_*}^{\varphi_{END}} \frac{1}{\sqrt{2\epsilon}} d\varphi \cong \sqrt{\frac{3\alpha}{4\epsilon_*}}, \qquad (7)$$

so we get the standard form of the spectral index and the tensor/scalar ratio for an α-attractor [45],

$$n_s \cong 1 - 6\epsilon_* + 2\eta_* \cong 1 - \frac{2}{N}, \qquad r \cong 16\epsilon_* \cong \frac{12\alpha}{N^2}. \qquad (8)$$

Finally, it is well known that the power spectrum of scalar perturbations is given by

$$\mathcal{P}_\zeta = \frac{H_*^2}{8\pi^2 \epsilon_* M_{pl}^2} \sim 2 \times 10^{-9} \qquad (9)$$

and, since in our case $V(\varphi_*) \cong \lambda M_{pl}^4 e^n$ and thus $H_*^2 \cong \frac{\lambda M_{pl}^2}{3} e^n$, taking into account that $\epsilon_* \cong \frac{3\alpha}{16}(1 - n_s)^2$, one gets the constraint

$$\lambda e^n / \alpha \sim 10^{-10}, \qquad (10)$$

where we have chosen as the value of n_s its central value given by the Planck team, i.e., $n_s = 0.9649$ [38].

Choosing, for example, $\alpha = 10^{-2}$, the constraint (10) becomes $\lambda e^n \sim 10^{-12}$. On the other hand, at the present time, we will have $\frac{\varphi_0}{\sqrt{6\alpha}M_{pl}} \gg 1$, where φ_0 denotes the current value of the inflaton field. Hence, we will have $V(\varphi_0) \sim \lambda M_{pl}^4 e^{-n}$, which is the dark energy at the present time, meaning that

$$0.7 \cong \Omega_{\varphi,0} \cong \frac{V(\varphi_0)}{3H_0^2 M_{pl}^2} \sim \frac{\lambda e^{-n}}{3} \left(\frac{M_{pl}}{H_0}\right)^2. \qquad (11)$$

Thus, taking, for example, the value provided by the Planck team [38,39], $H_0 = 67.81$ km/sec/Mpc $= 5.94 \times 10^{-61} M_{pl}$, we get the equations

$$\lambda e^n \sim 10^{-12} \quad \text{and} \quad \lambda e^{-n} \sim 10^{-120}, \tag{12}$$

the solutions of which are given by $n \sim 124$ and $\lambda \sim 10^{-66}$.

III. DYNAMICAL EVOLUTION OF THE SCALAR FIELD

The goal of this section is to calculate the value of the scalar field and its derivative at the reheating time. To do it, first of all we need to calculate the value of the inflaton field and its derivative at the beginning of kination [64,65], which could be calculated as follows: taking into account that the slow-roll regime is an attractor, we only need to take initial conditions in the basin of attraction of the slow-roll solution and thus integrate the conservation equation up to the moment that the effective EoS parameter was very close to 1, which is the moment when nearly all the energy density of the scalar field is kinetic.

So, we will take as initial condition the value of the inflaton when the pivot scale leaves the Hubble radius with vanishing temporal derivative (recall that during the slow roll the kinetic energy is negligible compared with the potential one). In this way, from Eq. (8), we get the relation

$$\epsilon_* = \frac{3\alpha}{16}(1 - n_s)^2, \tag{13}$$

which, together with the expression of ϵ_* given in (6), leads to the relation

$$\cosh\left(\frac{\varphi_*}{\sqrt{6\alpha}M_{pl}}\right) = \sqrt{\frac{2n}{3\alpha(1 - n_s)}}, \tag{14}$$

the solution of which is given by

$$\varphi_* = \sqrt{6\alpha}M_{pl} \ln\left(\sqrt{\frac{2n}{3\alpha(1 - n_s)}} - \sqrt{\frac{2n}{3\alpha(1 - n_s)} - 1}\right).$$

Finally, integrating numerically the conservation equation

$$\ddot{\varphi} + 3H\dot{\varphi} + V_{\varphi} = 0, \tag{15}$$

where $H = \frac{1}{\sqrt{3}M_{pl}}\sqrt{\frac{\dot{\varphi}^2}{2} + V(\varphi)}$ and with initial conditions $\varphi_i = \varphi_*$ and $\dot{\varphi}_i = 0$, we have obtained for the values $\alpha = 10^{-2}$, $n \cong 124$, and $n_s = 0.9649$ the following values at the beginning of the kination period: $\varphi_{\text{kin}} \cong 1.1M_{pl}$ and $\dot{\varphi}_{\text{kin}} \cong 6 \times 10^{-8}M_{pl}^2$.

When one has these values, analytical calculations can be done disregarding the potential during kination because in this epoch the potential energy of the field is negligible compared with the kinetic one. Then, since during kination one has $a \propto t^{1/3} \Rightarrow H = \frac{1}{3t}$, using the Friedmann equation, the dynamics in this regime will be obtained solving the equation

$$\frac{\dot{\varphi}^2}{2} = \frac{M_{pl}^2}{3t^2} \Rightarrow \dot{\varphi} = \sqrt{\frac{2}{3}}\frac{M_{pl}}{t} \Rightarrow$$

$$\varphi(t) = \varphi_{\text{kin}} + \sqrt{\frac{2}{3}}M_{pl} \ln\left(\frac{t}{t_{\text{kin}}}\right). \tag{16}$$

Thus, at the reheating time, i.e., at the beginning of the radiation era, one has

$$\varphi_{rh} = \varphi_{\text{kin}} + \sqrt{\frac{2}{3}}M_{pl} \ln\left(\frac{H_{\text{kin}}}{H_{rh}}\right). \tag{17}$$

By using that at the reheating time (i.e., when the energy density of the scalar field and the one of the relativistic plasma are of the same order) the Hubble rate is given by $H_{rh}^2 = \frac{2\rho_{rh}}{3M_{pl}^2}$, one gets

$$\varphi_{rh} = \varphi_{\text{kin}} + \sqrt{\frac{2}{3}}M_{pl} \ln\left(\frac{H_{\text{kin}}}{\sqrt{\frac{\pi^2 g_{rh}}{45}\frac{T_{rh}^2}{M_{pl}}}}\right)$$

$$\text{and} \quad \dot{\varphi}_{rh} = \sqrt{\frac{\pi^2 g_{rh}}{15}}T_{rh}^2, \tag{18}$$

where we have used that the energy density and the temperature are related via the formula $\rho_{rh} = \frac{\pi^2}{30}g_{rh}T_{rh}^4$, where the number of degrees of freedom for the standard model is $g_{rh} = 106.75$ [66].

Assuming instant preheating due to the smoothness of the potential [67–69], we will choose as the reheating temperature $T_{rh} \cong 10^9$ GeV because it is its natural value when this kind of mechanism is the responsible for reheating our Universe.

Then, at the beginning of the radiation era, we will have

$$\varphi_{rh} \cong 21.5M_{pl} \qquad \dot{\varphi}_{rh} \cong 1.41 \times 10^{-18}M_{pl}^2. \tag{19}$$

IV. NUMERICAL SIMULATION

To perform our numerical calculations, first of all, we consider the central values obtained in Ref. [37] (see the second column in Table IV) of the redshift at the matter-radiation equality $z_{\text{eq}} = 3365$; the present value of the ratio of the matter energy density to the critical one $\Omega_{m,0} = 0.308$; and, once again, $H_0 = 67.81$ km/ sec /Mpc $= 5.94 \times 10^{-61}M_{pl}$. Then, the present value of the matter energy density is $\rho_{m,0} = 3H_0^2 M_{pl}^2 \Omega_{m,0} = 3.26 \times 10^{-121}M_{pl}^4$, and at matter-radiation equality, we will have $\rho_{\text{eq}} = 2\rho_{m,0}(1 + z_{\text{eq}})^3 = 2.48 \times 10^{-110}M_{pl}^4 = 8.8 \times 10^{-1}$ eV^4. So, at the beginning of matter-radiation equality, the energy density of the matter and radiation will be $\rho_{m,\text{eq}} = \rho_{r,\text{eq}} = \rho_{\text{eq}}/2 \cong 4.4 \times 10^{-1}$ eV^4. Therefore, the dynamical equations after the beginning of the radiation can be easily

obtained using as a time variable $N \equiv -\ln(1+z) = \ln(\frac{a}{a_0})$. Recasting the energy density of radiation and matter, respectively, as a function of N, we get

$$\rho_m(a) = \rho_{m,\mathrm{eq}}\left(\frac{a_{\mathrm{eq}}}{a}\right)^3 \rightarrow \rho_m(N) = \rho_{m,\mathrm{eq}}e^{3(N_{\mathrm{eq}}-N)} \quad (20)$$

and

$$\rho_r(a) = \rho_{r,\mathrm{eq}}\left(\frac{a_{\mathrm{eq}}}{a}\right)^4 \rightarrow \rho_r(N) = \rho_{r,\mathrm{eq}}e^{4(N_{\mathrm{eq}}-N)}, \quad (21)$$

where $N_{\mathrm{eq}} \cong -8.121$ denotes the value of the time N at the beginning of the matter-radiation equality. The dynamical system for this scalar field model is obtained introducing the dimensionless variables

$$x = \frac{\varphi}{M_{pl}} \quad \text{and} \quad y = \frac{\dot\varphi}{H_0 M_{pl}}. \quad (22)$$

Thus, from the conservation equation $\ddot\varphi + 3H\dot\varphi + V_\varphi = 0$, one gets the dynamical system

$$\begin{cases} x' = y/\bar{H}, \\ y' = -3y - \bar{V}_x/\bar{H}, \end{cases} \quad (23)$$

where the prime is the derivative with respect to N, $\bar{H} = \frac{H}{H_0}$ and $\bar{V} = \frac{V}{H_0^2 M_{pl}^2}$. Note also that one can write

$$\bar{H} = \frac{1}{\sqrt{3}}\sqrt{\frac{y^2}{2} + \bar{V}(x) + \bar\rho_r(N) + \bar\rho_m(N)}, \quad (24)$$

where we have defined the dimensionless energy densities as $\bar\rho_r = \frac{\rho_r}{H_0^2 M_{pl}^2}$ and $\bar\rho_m = \frac{\rho_m}{H_0^2 M_{pl}^2}$. Finally, we have to integrate the dynamical system (23), with initial conditions $x(N_{rh}) = x_{rh} = 21.5$ and $y(N_{rh}) = y_{rh} = 2.42 \times 10^{42}$ imposing that

$\bar{H}(0) = 1$, which must be accomplished in order to ensure that the Hubble constant at the present time is the observed one, and where N_{rh} denotes the beginning of reheating, which is obtained imposing that

$$\rho_{r,\mathrm{eq}}e^{4(N_{\mathrm{eq}}-N_{rh})} = \frac{\pi^2}{30}g_{rh}T_{rh}^4, \quad (25)$$

that is,

$$N_{rh} = N_{\mathrm{eq}} - \frac{1}{4}\ln\left(\frac{g_{rh}}{g_{\mathrm{eq}}}\right) - \ln\left(\frac{T_{rh}}{T_{\mathrm{eq}}}\right) \cong -50.68, \quad (26)$$

where we have used that $\rho_{\mathrm{eq},r} = \frac{\pi^2}{30}g_{\mathrm{eq}}T_{\mathrm{eq}}^4$ with $g_{\mathrm{eq}} = 3.36$ [66] and thus $T_{\mathrm{eq}} \cong 7.81 \times 10^{-10}$ GeV. The obtained results are presented in Fig. 1, where one can see the similitude with the recent results obtained in Ref. [63] dealing with Lorentzian quintessential inflation.

The Planck team [38] provided the following value of the dark energy EoS parameter at the present time, $w_{de,0} = -1.03 \pm 0.03$. So, since the effective EoS parameter is given by

$$w_{\mathrm{eff}} = \frac{1}{3}\Omega_r + w_{de}\Omega_{de}, \quad (27)$$

taking into account that the present value of Ω_r is approximately 0.0001 and $\Omega_{de,0} \cong 0.69$, one gets at 1σ C.L. that $w_{\mathrm{eff}} = -0.712 \pm 0.021$; i.e., at 2σ C.L., we have $-0.754 \leq w_{\mathrm{eff},0} \leq -0.67$, which is compatible with our model, as one can see on the right-hand side of Fig. 1. In fact, in our case, we have obtained $w_{\mathrm{eff},0} \cong -0.68$.

V. OBSERVATIONAL CONSTRAINTS

Next, we describe the observational datasets along with the relevant statistics in constraining the model. The dataset incorporates few different measurements.
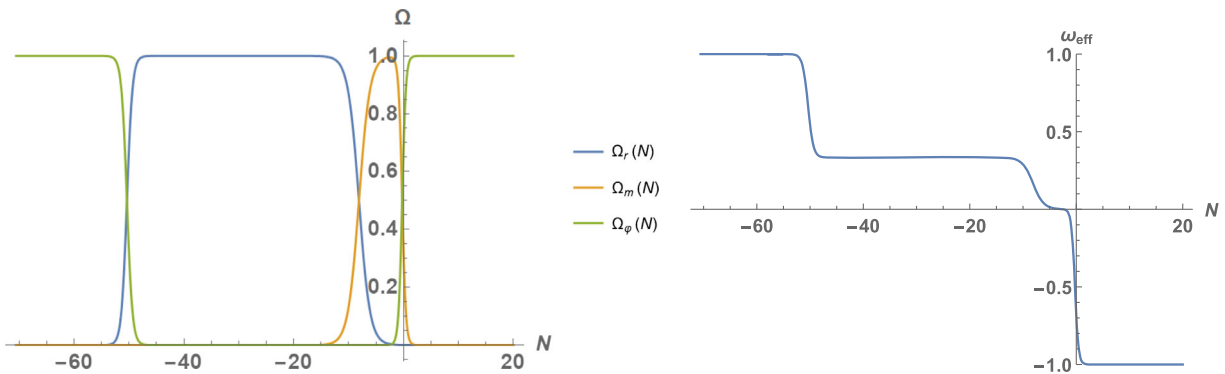
FIG. 1. Left: the density parameters $\Omega_m = \frac{\rho_m}{3H^2 M_{pl}^2}$ (orange curve), $\Omega_r = \frac{\rho_r}{3H^2 M_{pl}^2}$ (blue curve), and $\Omega_\varphi = \frac{\rho_\varphi}{3H^2 M_{pl}^2}$, from kination to future times. Right: The effective equation of state parameter w_{eff}, from kination to future times. As one can see in the picture, after kination, the Universe enters in a large period of time where radiation dominates. Then, after the matter-radiation equality, the Universe becomes matter dominated, and, finally, near the present, it enters in a new accelerated phase where w_{eff} approaches -1.

A. Direct measurements of the Hubble expansion

1. Cosmic chronometers

The dataset exploits the evolution of differential ages of passive galaxies at different redshifts to directly constrain the Hubble parameter [70]. We use uncorrelated 30 CC measurements of $H(z)$ discussed in Refs. [71–74]. Here, the corresponding χ_H^2 function reads

$$\chi_H^2 = \sum_{i=1}^{30} \left(\frac{H_i - H_{\text{pred}}(z_i)}{\Delta H_i} \right)^2, \qquad (28)$$

where H_i is the observed Hubble rates at redshift z_i $(i = 1, …, N)$ and H_{pred} is the predicted one from the model.

B. Standard candles

As standard candles (SCs), we use measurements of the Pantheon Type Ia supernova (SnIa) [75]. The model parameters of the models are to be fitted with by comparing the observed μ_i^{obs} value to the theoretical μ_i^{th} value of the distance moduli which are the logarithms

$$\mu = m - M = 5 \log_{10}(D_L) + \mu_0, \qquad (29)$$

where m and M are the apparent and absolute magnitudes and $\mu_0 = 5 \log (H_0^{-1}/\text{Mpc}) + 25$ is the nuisance parameter that has been marginalized. The luminosity distance is defined by

$$D_L(z) = \frac{c}{H_0} (1 + z) \int_0^z \frac{dz^*}{E(z^*)}. \qquad (30)$$

Here, $\Omega_k = 0$ (flat spacetime). Following standard lines, the chi-square function of the standard candles is given by

$$\chi_{\text{SC}}^2(\phi_s^\nu) = \mu_s \mathbf{C}_{s,\text{cov}}^{-1} \mu_s^T, \qquad (31)$$

where $\mu_s = \{\mu_1 - \mu_{\text{th}}(z_1, \phi^\nu), …, \mu_N - \mu_{\text{th}}(z_N, \phi^\nu)\}$ and the subscript s denotes SnIa and quasars. For the SnIa data, the covariance matrix is not diagonal, and the distance modulus is given as $\mu_i = \mu_{B,i} - \mathcal{M}$, where $\mu_{B,i}$ is the maximum apparent magnitude in the rest frame for redshift z_i and $\mathcal{M}$ is treated as a universal free parameter [75], quantifying various observational uncertainties. It is apparent that $\mathcal{M}$ and h parameters are intrinsically degenerate in the context of the Pantheon dataset, so we cannot extract any information regarding H_0 from SnIa data alone.

C. Baryon acoustic oscillations

We use uncorrelated data points from different baryon acoustic oscillations (BAOs). BAOs are a direct consequence of the strong coupling between photons and baryons in the prerecombination epoch. After the decoupling of photons, the overdensities in the baryon fluid evolved and attracted more matter, leaving an imprint in the two-point correlation function of matter fluctuations with a characteristic scale of around $r_d \approx 147$ Mpc that can be used as a standard ruler and to constrain cosmological models. Studies of the BAO feature in the transverse direction provide a measurement of $D_H(z)/r_d = c/H(z)r_d$, with the comoving angular diameter distance being [76,77]

$$D_M = \int_0^z \frac{c\,dz'}{H(z')}. \qquad (32)$$

The angular diameter distances $D_A = D_M/(1 + z)$ and $D_V(z)/r_d$ are a combination of the BAO peak coordinates above, namely,

$$D_V(z) \equiv [zD_H(z)D_M^2(z)]^{1/3}. \qquad (33)$$

The surveys provide the values of the measurements at some effective redshift. We employ the following BAO data points, collected in Ref. [78] from Refs. [79–90], in the redshift range $0.106 < z < 2.34$. Since Ref. [78] proves the uncorrelation of this dataset,

$$\chi_{\text{BAO}}^2 = \sum_{i=1}^{17} \left(\frac{D_i - D_{\text{pred}}(z_i)}{\Delta D_i} \right)^2, \qquad (34)$$

where D_i is the observed distant module rates at redshift z_i $(i = 1, …, N)$ and D_{pred} is the predicted one from the model.

D. Cosmic microwave background

Finally, we take the cosmic microwave background (CMB) distant prior measurements [91]. The distance priors provide effective information of the CMB power spectrum in two aspects: the acoustic scale l_A characterizes the CMB temperature power spectrum in the transverse direction, leading to the variation of the peak spacing, and the "shift parameter" R influences the CMB temperature spectrum along the line-of-sight direction, affecting the heights of the peaks, which are defined as

$$l_A = (1 + z_d) \frac{\pi D_A(z_d)}{r_d},$$

$$R(z_d) = \frac{\sqrt{\Omega_m} H_0}{c} (1 + z_d) D_A(z_d), \qquad (35)$$

with its corresponding covariance matrix (see Table I in Ref. [91]). The BAO scale is set by the sound horizon at the drag epoch $z_d \approx 1060$ when photons and baryons decouple, given by

$$r_d = \int_{z_d}^\infty \frac{c_s(z)}{H(z)} dz, \qquad (36)$$

where $c_s \approx c(3 + 9\rho_b/(4\rho_\gamma))^{-0.5}$ is the speed of sound in the baryon-photon fluid with the baryon and photon densities being $\rho_b(z)$ and $\rho_\gamma(z)$, respectively [92]. However, in our analysis, we used r_d as an independent parameter. The χ^2_{CMB} is defined in Ref. [91].

We include the latest measurement of the Hubble parameter

$$H_0 = (73.2 \pm 1.3) \text{ km/s/Mpc} \tag{37}$$

reported by Ref. [93]. The measurement presents an expanded sample of 75 Milky Way Cepheids with Hubble Space Telescope photometry and Gaia EDR3 parallaxes which uses the extragalactic distance ladder in order to recalibrate and refine the determination of the Hubble constant. The combination is related via the relation

$$\chi^2_{\text{Hub}} = \left(\frac{H_0 - 73.2}{1.3}\right)^2. \tag{38}$$

The χ^2_{Hub} estimates the deviation from the latest measurement of the Hubble constant.

E. Joint analysis and model selection

To perform a joint statistical analysis of four cosmological probes, we need to use the total likelihood function; consequently, the χ^2_{tot} expression is given by

$$\chi^2_{\text{tot}} = \chi^2_{\text{CMB}} + \chi^2_H + \chi^2_{\text{SC}} + \chi^2_{\text{BAO}} + \chi^2_{\text{Hub}}. \tag{39}$$

Regarding the problem of likelihood maximization, we use an affine-invariant Markov chain Monte Carlo sampler [94], as it is implemented within the open-source package POLYCHORD [95] with the GETDIST package [96] to present the results. The prior we choose is with a uniform distribution, where $\Omega_m \in [0.; 1.]$, $\Omega_{de} \in [0.; 1 - \Omega_m]$, $\Omega_r \in [0.; 1 - \Omega_m - \Omega_{de}]$, $H_0 \in [50; 100]$ km/ sec /Mpc, and $r_d \in [130; 160]$ Mpc. For the scalar field final condition, we imposed $\phi \in [20; 25]$.

Furthermore, we use the logarithmic Bayes factor defined as

$$\log(B_{01}) = \log(Z_0) - \log(Z_1), \tag{40}$$

where Z_i is the logarithmic marginalized evidence reported by POLYCHORD [97]. For the logarithmic Bayes factor, a difference of $\log(B_{01}) \in [1/2, 1]$ is substantial in favor of Z_0, $\log(B_{01}) \in [1, 2]$ is strong, and $\log(B_{01}) > 2$ is decisive. In the case of negative values, the same applies for Z_1.

F. Results

Figure 2 shows the posterior distribution of the data fit with the best-fit values at Table I. The posterior one for the additional parameters is described in Fig. 3. The

quintessential α-attractor inflation (QαI) model is a viable model and can describe early times as well as late times. Actually, there is no distinguishable difference between the ΛCDM fit and the QαI, since the potential in that regime includes a slow-roll behavior. In conclusion, this model includes the inflationary period and predicts the large difference between the inflationary and the late dark energy, while the standard models do not predict that. But also for the measurements from the observed Universe, there is no distinguishable difference between the standard models and the QαI model.

To complete our analysis, we use the Bayesian evidence. The difference between the models yields $\Delta B_{ij} = 1.11$, which implies a slight preference for the ΛCDM model. It seems that the difference is due to the additional parameters that the model suggests. However, as we said, this additional parameter gives a natural explanation for the dark energy differences. But statistically, there is a slight preference for the ΛCDM model.

VI. α-ATTRACTORS WITH A FINE-TUNED COSMOLOGICAL CONSTANT

In this section, we review the treatment of α-attractor done in Ref. [59]. First of all, one has to introduce a CC with the form $\Lambda = \lambda M_{pl}^2 e^{-n}$, and thus, adding to the Lagrangian the term ΛM_{pl}^2 leads to the following effective potential:

$$V(\varphi) = \lambda M_{pl}^4 e^{-n} \left(e^{n(1 - \tanh(\frac{\varphi}{\sqrt{6\alpha}M_{pl}}))} - 1 \right). \tag{41}$$

During inflation, $\varphi < 0$, and the potential becomes as (3) because $e^{-n} \ll 1$. So, as we have shown for the potential (3), for small values of α, inflation works also well when this CC is introduced in the model.

In the same way, for large values of the scalar field, the potential will become

$$V(\varphi) = 2n\lambda e^{-n} M_{pl}^4 e^{-\gamma\varphi/M_{pl}}, \tag{42}$$

with $\gamma \equiv \sqrt{\frac{2}{3\alpha}}$. It is well known [98,99] that for an exponential potential a late-time eternal acceleration is achieved when $\gamma < \sqrt{2}$, that is, for $\alpha > 1/3$. Effectively, as has been shown in Ref. [54], by introducing the dimensionless variables

$$\tilde{x} \equiv \frac{\dot{\varphi}}{\sqrt{6}M_{pl}H} \quad \text{and} \quad \tilde{y} \equiv \frac{\sqrt{V}}{\sqrt{3}M_{pl}H}, \tag{43}$$

after the matter-radiation equality, the dynamical system (23) can be written as
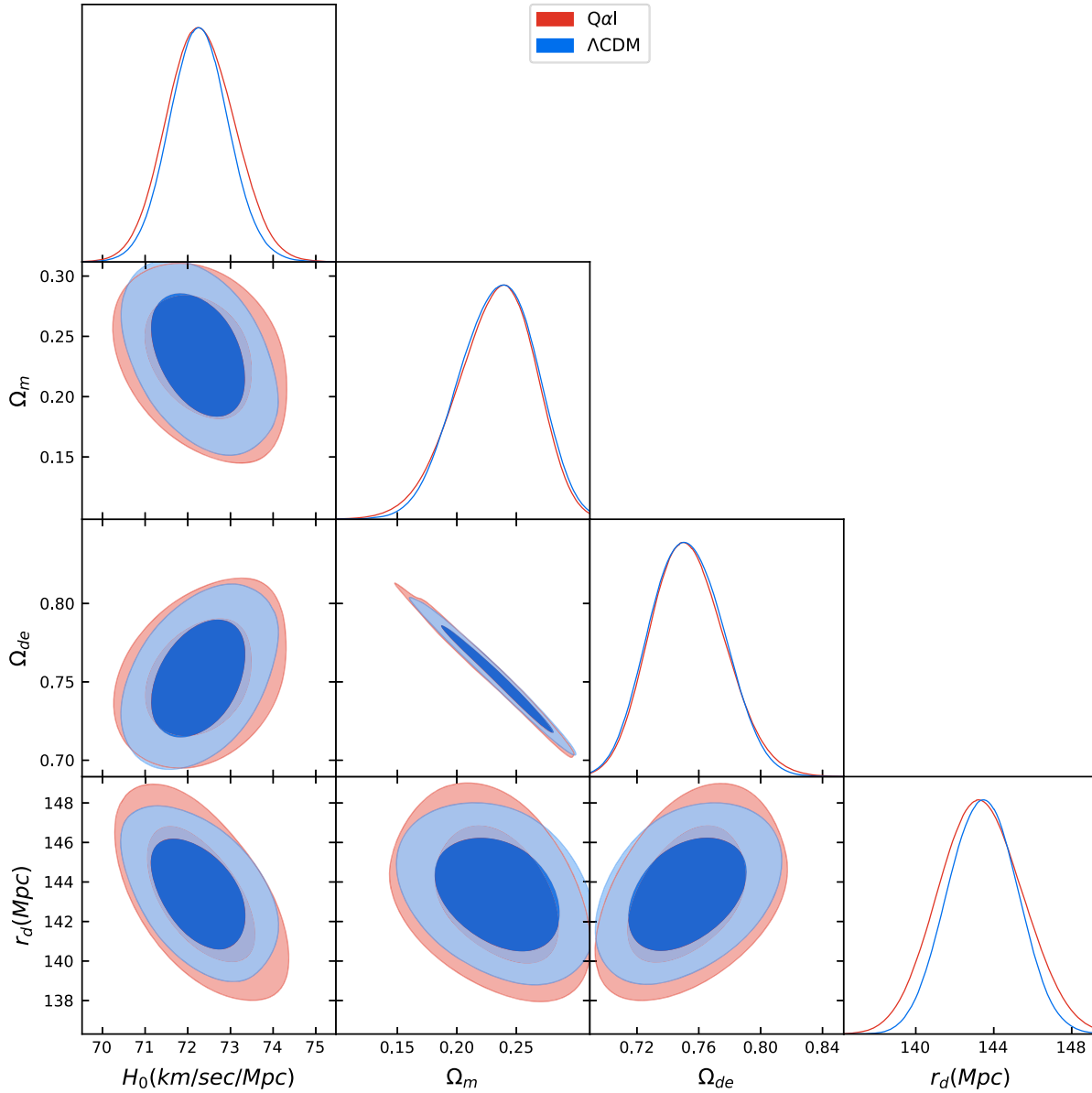
FIG. 2.   The posterior distribution for different measurements with the quintessential α-attractor inflation (QαI) model with 1σ and 2σ for Ω_m, Ω_{de}, H_0, and r_d.

TABLE I.   The best-fit values for the discussed model. The values φ_0 and $\dot{\varphi}_0$ denote the current values of the scalar field and its derivative.

Parameter	QαI	ΛCDM
$H_0(\text{km/ sec /Mpc})$	72.25 ± 0.74	72.24 ± 0.65
φ_0/M_{pl}	22.46 ± 1.419	$\cdots$
$\dot{\varphi}_0/(H_0 M_{pl})10^{-71}$	5.09 ± 2.858	$\cdots$
Ω_m	0.2323 ± 0.0286	0.2393 ± 0.02751
Ω_{de}	0.7535 ± 0.02092	0.7489 ± 0.2027
n	122.1 ± 2.021	$\cdots$
α	0.2760 ± 0.1448	$\cdots$
$r_d(\text{Mpc})$	143.4 ± 1.941	143.5 ± 1.577
B_{ij}	-80.54	-79.43

$$\begin{cases} \tilde{x}' = -3\tilde{x} + \sqrt{\frac{3}{2}}\gamma\tilde{y}^2 + \frac{3}{2}\tilde{x}[\tilde{x}^2 - \tilde{y}^2 + 1] \\ \tilde{y}' = -\sqrt{\frac{3}{2}}\gamma\tilde{x}\,\tilde{y} + \frac{3}{2}\tilde{y}[\tilde{x}^2 - \tilde{y}^2 + 1], \end{cases} \quad (44)$$

together with the constraint

$$\tilde{x}^2 + \tilde{y}^2 + \Omega_m = 1. \quad (45)$$

The system (44) has the following fixed point $\tilde{x} = \frac{\gamma}{\sqrt{6}}$ and $\tilde{y} = \sqrt{1 - \frac{\gamma^2}{6}}$, which depicts an attractor (tracker) solution with $w_{\text{eff}} = \tilde{x}^2 - \tilde{y}^2 = \frac{\gamma^2}{3} - 1$ and $\Omega_\varphi = 1$. For this reason, if one demands an accelerated period at late times, one has
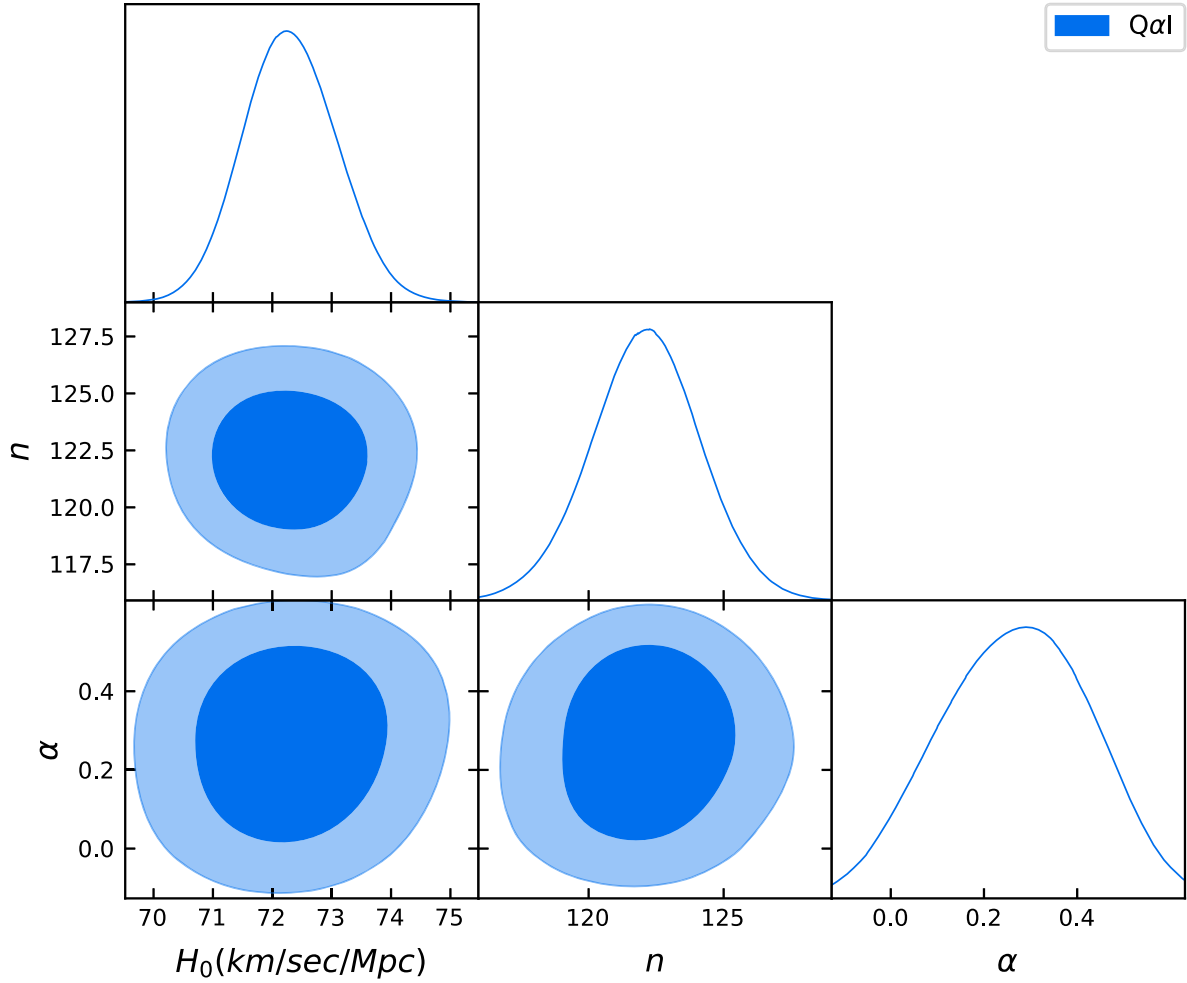
FIG. 3. The posterior distribution for the QαI model with 1σ and 2σ C.L., for the Hubble parameter vs the parameter n and α. The dataset include baryon acoustic oscillations dataset, cosmic chronometers, the Hubble diagram from Type Ia supernova, and the CMB.

to choose $\gamma^2 < 2$, as seen in Fig. 4 for the case $\gamma = 0.277$. In addition, as has been shown in Ref. [54], this tracker solution is given by

$$\varphi_{tra}(N) = -\frac{n}{\gamma}M_{pl} + NM_{pl} + \frac{M_{pl}}{\gamma}\ln\left(\frac{4n\lambda}{(6-\gamma)^2}\right)$$
$$+ \frac{2M_{pl}}{\gamma}\ln\left(\frac{M_{pl}}{H_0}\right). \tag{46}$$

However, since in this case one has to choose $\alpha > 1/3$, the calculation of the spectral index and the ratio of tensor to scalar perturbations changes a little bit with respect to the case $\alpha \ll 1$, obtaining (see Ref. [59] for details)

$$n_s \cong 1 - \frac{2}{N + \frac{\sqrt{3\alpha}}{2}}, \qquad r = \frac{12\alpha}{(N + \frac{\sqrt{3\alpha}}{2})^2}. \tag{47}$$

To end with the case $\gamma \leq \sqrt{2}$, we have numerically checked that, in order to obtain at the present time an effective EoS

parameter compatible with the Planck data, there is a very narrow range of values of α, as is shown in Fig. 4. In fact, the only value which might be considered viable is $\gamma \cong 0.277 \Leftrightarrow \alpha \cong 8.688$, which lies very close to the lower bound of the 2σ C.L. of the allowed values. So, this is not at all sufficient to prove or disprove the viability of the CC model.

On the other hand, in the case $\gamma > \sqrt{3} \Rightarrow \alpha < 2/9$, the dynamical system (44) has another fixed point, namely, $\tilde{x} = \tilde{y} = \sqrt{\frac{3}{2}\frac{1}{\gamma}}$, which corresponds to a matter-dominated Universe because $w_{\text{eff}} = 0$. In that case, it is argued in Ref. [59] that, when $\sqrt{3} < \gamma < 2\sqrt{6} \Rightarrow 1/36 < \alpha < 2/9$, the scalar field may dominate for a brief period, obtaining a short period of acceleration. However, we have not been able to find the numerical values of the parameters λ and n satisfying the constraint $\lambda e^n/\alpha \sim 10^{-10}$ provided by the power spectrum of scalar perturbations and the essential identity $\bar{H}(0) = 1$ at the present time. That is, when one adds this cosmological constant, for values of α less than $2/9$, from our viewpoint, it is impossible to unify the early- and late-time acceleration of our Universe.
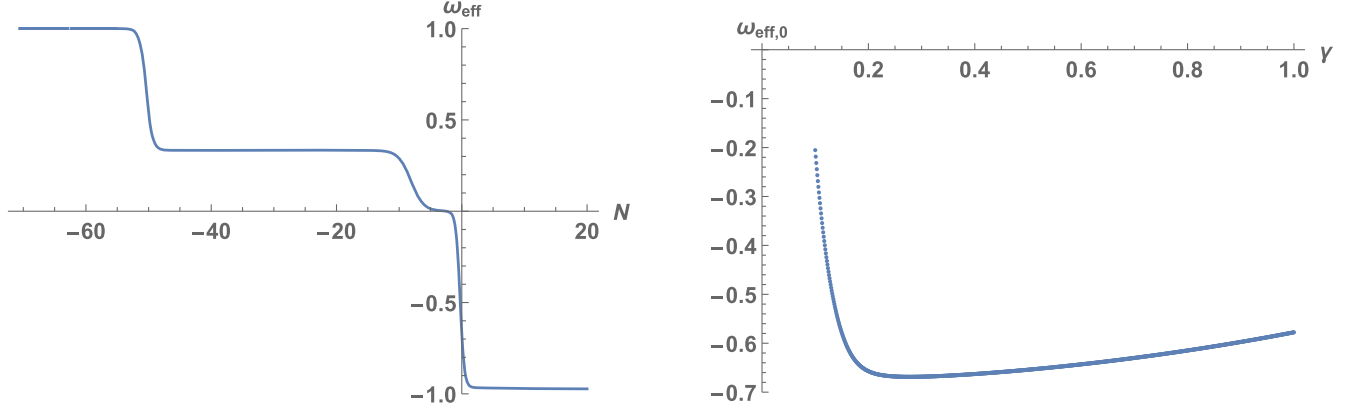
FIG. 4.   Left: evolution of the equation of state parameter w_{eff} from the kination phase to late times for $\gamma = 0.277$ according to the system (44), taking as initial conditions the ones obtained from the numerical simulation carried out in Sec. IV. We see that w_{eff} is 1 during the kination phase that takes place in quintessential inflation models after inflation. Then, reheating occurs, and w_{eff} becomes $1/3$, which is maintained during all the radiation phase until the matter-radiation equality. And then, it finally effectively converges to $\gamma^2/3 - 1$, obtaining an eternal accelerating Universe. Right: equation of state parameter at the present time for different set of values of $0 < \gamma < \sqrt{2}$. All of them lie outside of the 2σ C.L. Planck observational data, including $\gamma = 0.277$ with $w_{\text{eff},0} = -0.669$, though this value lies very close to it.

VII. POWER-LAW POTENTIALS

In the Lagrangian (1), one can replace the exponential potential by a power law with the form

$$V_s(\phi) = \lambda M_{pl}^4 \left(1 - e^{-\beta} \frac{\phi}{\sqrt{6\alpha}} \right)^s, \qquad (48)$$

where λ, β, and α are positive dimensionless variables and s is an odd number. We also assume that β is close to zero. Then, in terms of the scalar field φ, the potential becomes

$$V_s(\varphi) = \lambda M_{pl}^4 \left(1 - e^{-\beta} \tanh\left(\frac{\varphi}{\sqrt{6\alpha} M_{pl}} \right) \right)^s, \quad (49)$$

which, for small values of α, belongs to the class of α-attractors (see, for instance, Ref. [47]).

To obtain the value of the parameters λ and β, we follow the same method as in Sec. II, getting

$$2^s \lambda/\alpha \sim 10^{-10}, \qquad \lambda(1 - e^{-\beta})^s \sim 10^{-120}. \quad (50)$$

Choosing, for example, $\alpha \sim 10^{-2}$, we get

$$\lambda \sim 10^{-12} 2^{-s} \quad \text{and} \quad \beta \sim -\ln(1 - 2 \times 10^{-108/s}), \quad (51)$$

which, for $s = 1$ leads to

$$\lambda \sim 5 \times 10^{-13} \quad \text{and} \quad \beta \sim 2 \times 10^{-108}, \qquad (52)$$

for $s = 3$ to

$$\lambda \sim 1.25 \times 10^{-13} \quad \text{and} \quad \beta \sim 2 \times 10^{-36}, \qquad (53)$$

and so on.

Then, since for small values of s one has $\beta \cong 0$, we can safely assume that $\beta = 0$, and the potential becomes $V_s(\varphi) = \lambda M_{pl}^4 (1 - \tanh(\frac{\varphi}{\sqrt{6\alpha} M_{pl}}))^s$, which for large values of the scalar field (which happens at the present time) has the exponential form

$$V_s(\varphi) \cong 2^s \lambda M_{pl}^4 e^{-\frac{2s\varphi}{\sqrt{6\alpha} M_{pl}}} \cong \alpha 10^{-10} M_{pl}^4 e^{-\gamma \varphi/M_{pl}}, \quad (54)$$

where now $\gamma = \sqrt{\frac{2}{3\alpha}} s$. Thus, as we have already commented in Sec. VI, in order to have an accelerated expansion at late times, the value of γ must be smaller than $\sqrt{2}$; that is, one has to choose $\alpha > s^2/3$. In fact, to agree with the Planck observational data, one has to choose the parameter α to satisfy, at the present time, $w_{\text{eff},0} = -0.712 \pm 0.03$.

Unfortunately, in these power-law models, inflation never ends. Effectively, choosing for simplicity $s = 1$, the main slow-roll parameter is given by

$$\epsilon = \frac{1}{12\alpha} \frac{1}{\cosh^4(\frac{\varphi}{\sqrt{6\alpha} M_{pl}})} \frac{1}{(1 - \tanh(\frac{\varphi}{\sqrt{6\alpha} M_{pl}}))^2}$$

$$= \frac{1}{12\alpha} \left(1 + \tanh\left(\frac{\varphi}{\sqrt{6\alpha} M_{pl}} \right) \right)^2. \qquad (55)$$

Thus, at the end of inflation ($\epsilon = 1$), we will have

$$\tanh\left(\frac{\varphi_{END}}{\sqrt{6\alpha}M_{pl}}\right) = -1 + \sqrt{12\alpha}, \qquad (56)$$

which does not have solution for $\alpha > 1/3$. Therefore, we can conclude that these power-law potentials must be disregarded.

VIII. CONCLUDING REMARKS

We have studied different quintessential inflation potentials such as exponential or power-law potentials in the context of α-attractors. We have shown that the potential which provides the best results compatible with the current observational data is the exponential one without any kind of cosmological constant. In fact, the behavior of the dynamics provided by an exponential α-attractor potential is very similar to the dynamics in the so-called Lorentzian quintessential inflation, where at very late times the effective EoS parameter converges to -1.

We have also verified that this model fits statistically very well with the observational datasets coming from Type Ia supernova, cosmic microwave background, and the cosmic chronometers. The QαI model is a viable model from the data fit. There is a slight preference for the ΛCDM model from the Bayesian evidence. However, this model still unifies naturally inflationary and late-time dark energy behavior and explains the difference between the energy density values from these epochs.

On the contrary, the introduction of a cosmological constant leads for values of the parameter α greater than $1/3$, at the present time, to an effective EoS parameter that does not enter at the 2σ C.L., in the region provided by the Planck team, and even worse, for $\alpha < 2/9$, the model is unable to depict both the early- and late-time acceleration of the Universe. In addition, for power-law potentials, in the context of α-attractors, the inflationary regime never finishes, which invalidates its viability.

[1] A. H. Guth, Phys. Rev. D **23,** 347 (1981); Adv. Ser. Astrophys. Cosmol. **3,** 139 (1987).

[2] A. H. Guth and S. Y. Pi, Phys. Rev. Lett. **49,** 1110 (1982).

[3] A. A. Starobinsky, JETP Lett. **30,** 682 (1979); **30,** 767 (1979).

[4] D. Kazanas, Astrophys. J. **241,** L59 (1980).

[5] A. A. Starobinsky, Phys. Lett. **91B,** 99 (1980); **91B,** 771 (1980).

[6] A. D. Linde, Phys. Lett. **108B,** 389 (1982); Adv. Ser. Astrophys. Cosmol. **3,** 149 (1987).

[7] A. Albrecht and P. J. Steinhardt, Phys. Rev. Lett. **48,** 1220 (1982); Adv. Ser. Astrophys. Cosmol. **3,** 158 (1987).

[8] J. D. Barrow and A. C. Ottewill, J. Phys. A **16,** 2757 (1983).

[9] S. K. Blau, E. I. Guendelman, and A. H. Guth, Phys. Rev. D **35,** 1747 (1987).

[10] J. D. Barrow and A. Paliathanasis, Phys. Rev. D **94,** 083518 (2016).

[11] J. D. Barrow and A. Paliathanasis, Gen. Relativ. Gravit. **50,** 82 (2018).

[12] K. A. Olive, Phys. Rep. **190,** 307 (1990).

[13] A. D. Linde, Phys. Rev. D **49,** 748 (1994).

[14] A. R. Liddle, P. Parsons, and J. D. Barrow, Phys. Rev. D **50,** 7222 (1994).

[15] C. Germani and A. Kehagias, Phys. Rev. Lett. **105,** 011302 (2010).

[16] T. Kobayashi, M. Yamaguchi, and J. Yokoyama, Phys. Rev. Lett. **105,** 231302 (2010).

[17] C.-J. Feng, X.-Z. Li, and E. N. Saridakis, Phys. Rev. D **82,** 023526 (2010).

[18] C. Burrage, C. de Rham, D. Seery, and A. J. Tolley, J. Cosmol. Astropart. Phys. 01 (**2011**) 014.

[19] T. Kobayashi, M. Yamaguchi, and J. Yokoyama, Prog. Theor. Phys. **126,** 511 (2011).

[20] J. Ohashi and S. Tsujikawa, J. Cosmol. Astropart. Phys. 10 (2012) 035.

[21] Y.-F. Cai, J.-O. Gong, S. Pi, E. N. Saridakis, and S.-Y. Wu, Nucl. Phys. **B900,** 517 (2015).

[22] V. Kamali, S. Basilakos, and A. Mehrabi, Eur. Phys. J. C **76,** 525 (2016).

[23] D. Benisty and E. I. Guendelman, Int. J. Mod. Phys. A **33,** 1850119 (2018).

[24] C. Middleton, B. A. Brouse, and S. D. Jackson, Eur. Phys. J. C **79,** 982 (2019).

[25] I. Dalianis, A. Kehagias, and G. Tringas, J. Cosmol. Astropart. Phys. 01 (2019) 037.

[26] I. Dalianis and G. Tringas, Phys. Rev. D **100,** 083512 (2019).

[27] T. Qiu, T. Katsuragawa, and S. Ni, Eur. Phys. J. C **80,** 1163 (2020).

[28] S. Choudhury, J. High Energy Phys. 04 (2014) 105.

[29] S. Choudhury and A. Mazumdar, Nucl. Phys. **B882,** 386 (2014).

[30] S. Choudhury and S. Pal, Phys. Rev. D **85,** 043529 (2012).

[31] S. Choudhury, A. Mazumdar, and S. Pal, J. Cosmol. Astropart. Phys. 07 (2013) 041.

[32] S. Choudhury, A. Mazumdar, and E. Pukartas, J. High Energy Phys. 04 (2014) 077.

[33] S. Choudhury, Eur. Phys. J. C **77,** 469 (2017).

[34] A. Banerjee, H. Cai, L. Heisenberg, E. O. Colgáin, M. M. Sheikh-Jabbari, and T. Yang, Phys. Rev. D **103,** L081305 (2021).

[35] A. A. Starobinsky, Phys. Lett. **91B,** 99 (1980); **91B,** 771 (1980).

[36] A. Kehagias, A. Moradinezhad Dizgah, and A. Riotto, Phys. Rev. D **89,** 043527 (2014).

[37] P. A. R. Ade et al. (Planck Collaboration), Astron. Astrophys. **594,** A13 (2016).

[38] Y. Akrami et al. (Planck Collaboration), Astron. Astrophys. **641,** A10 (2020).

[39] N. Aghanim et al. (Planck Collaboration), Astron. Astrophys. **641,** A6 (2020).

[40] A. Linde, J. Cosmol. Astropart. Phys. 05 (2015) 003.

[41] R. Kallosh, A. Linde, and D. Roest, J. High Energy Phys. 11 (2013) 198.

[42] R. Kallosh and A. Linde, J. Cosmol. Astropart. Phys. 12 (2013) 006.

[43] R. Kallosh, A. Linde, and D. Roest, Phys. Rev. Lett. **112,** 011303 (2014).

[44] S. Cecotti and R. Kallosh, J. High Energy Phys. 05 (2014) 114.

[45] R. Kallosh and A. Linde, Phys. Rev. D **91,** 083528 (2015).

[46] S. Ferrara, R. Kallosh, A. Linde, and M. Porrati, Phys. Rev. D **88,** 085038 (2013).

[47] R. Kallosh and A. Linde, J. Cosmol. Astropart. Phys. 07 (2013) 002.

[48] G. Cañas Herrera and F. Renzi, arXiv:2104.06398.

[49] P. J. E. Peebles and A. Vilenkin, Phys. Rev. D **59,** 063505 (1999).

[50] K. Dimopoulos and J. W. F. Valle, Astropart. Phys. **18,** 287 (2002).

[51] C.-Q. Geng, M. W. Hossain, R. Myrzakulov, M. Sami, and E. N. Saridakis, Phys. Rev. D **92,** 023522 (2015).

[52] C.-Q. Geng, C.-C. Lee, M. Sami, E. N. Saridakis, and A. A. Starobinsky, J. Cosmol. Astropart. Phys. 06 (2017) 011.

[53] M. W. Hossain, R. Myrzakulov, M. Sami, and E. N. Saridakis, Phys. Rev. D **89,** 123513 (2014).

[54] J. Haro, J. Amorós, and S. Pan, Eur. Phys. J. C **79,** 505 (2019).

[55] J. de Haro, J. Amorós, and S. Pan, Phys. Rev. D **93,** 084018 (2016).

[56] J. De Haro and L. Aresté Saló, Phys. Rev. D **95,** 123501 (2017).

[57] L. Aresté Saló and J. de Haro, Eur. Phys. J. C **77,** 798 (2017).

[58] E. Guendelman, R. Herrera, P. Labrana, E. Nissimov, and S. Pacheva, Gen. Relativ. Gravit. **47,** 10 (2015).

[59] K. Dimopoulos and C. Owen, J. Cosmol. Astropart. Phys. 06 (2017) 027.

[60] Y. Akrami, R. Kallosh, A. Linde, and V. Vardanyan, J. Cosmol. Astropart. Phys. 06 (**2018**) 041.

[61] D. Benisty and E. I. Guendelman, Eur. Phys. J. C **80,** 577 (2020).

[62] D. Benisty and E. I. Guendelman, Int. J. Mod. Phys. D **29,** 2042002 (2020).

[63] L. Aresté Saló, D. Benisty, E. I. Guendelman, and J. d. Haro, arXiv:2102.09514.

[64] M. Joyce, Phys. Rev. D **55,** 1875 (1997).

[65] B. Spokoiny, Phys. Lett. B **315,** 40 (1993).

[66] T. Rehagen and G. B. Gelmini, J. Cosmol. Astropart. Phys. 06 (2015) 039.

[67] G. N. Felder, L. Kofman, and A. D. Linde, Phys. Rev. D **59,** 123523 (1999).

[68] G. N. Felder, L. Kofman, and A. D. Linde, Phys. Rev. D **60,** 103505 (1999).

[69] J. Haro, Phys. Rev. D **99,** 043510 (2019).

[70] R. Jimenez and A. Loeb, Astrophys. J. **573,** 37 (2002).

[71] M. Moresco, L. Verde, L. Pozzetti, R. Jimenez, and A. Cimatti, J. Cosmol. Astropart. Phys. 07 (2012) 053.

[72] M. Moresco et al., J. Cosmol. Astropart. Phys. 08 (2012) 006.

[73] M. Moresco, Mon. Not. R. Astron. Soc. **450,** L16 (2015).

[74] M. Moresco, L. Pozzetti, A. Cimatti, R. Jimenez, C. Maraston, L. Verde, D. Thomas, A. Citro, R. Tojeiro, and D. Wilkinson, J. Cosmol. Astropart. Phys. 05 (2016) 014.

[75] D. Scolnic et al., Astrophys. J. **859,** 101 (2018).

[76] N. B. Hogg, M. Martinelli, and S. Nesseris, J. Cosmol. Astropart. Phys. 12 (2020) 019.

[77] M. Martinelli et al. (EUCLID Collaboration), Astron. Astrophys. **644,** A80 (2020).

[78] D. Benisty and D. Staicova, Astron. Astrophys. **647,** A38 (2021).

[79] W. J. Percival et al. (SDSS Collaboration), Mon. Not. R. Astron. Soc. **401,** 2148 (2010).

[80] F. Beutler, C. Blake, M. Colless, D. H. Jones, L. Staveley-Smith, L. Campbell, Q. Parker, W. Saunders, and F. Watson, Mon. Not. R. Astron. Soc. **416,** 3017 (2011).

[81] N. G. Busca et al., Astron. Astrophys. **552,** A96 (2013).

[82] L. Anderson et al., Mon. Not. R. Astron. Soc. **427,** 3435 (2012).

[83] H.-J. Seo et al., Astrophys. J. **761,** 13 (2012).

[84] A. J. Ross, L. Samushia, C. Howlett, W. J. Percival, A. Burden, and M. Manera, Mon. Not. R. Astron. Soc. **449,** 835 (2015).

[85] R. Tojeiro et al., Mon. Not. R. Astron. Soc. **440,** 2222 (2014).

[86] J. E. Bautista et al., Astrophys. J. **863,** 110 (2018).

[87] E. de Carvalho, A. Bernui, G. C. Carvalho, C. P. Novaes, and H. S. Xavier, J. Cosmol. Astropart. Phys. 04 (2018) 064.

[88] M. Ata et al., Mon. Not. R. Astron. Soc. **473,** 4773 (2018).

[89] T. M. C. Abbott et al. (DES Collaboration), Mon. Not. R. Astron. Soc. **483,** 4866 (2019).

[90] Z. Molavi and A. Khodam-Mohammadi, Eur. Phys. J. Plus **134,** 254 (2019).

[91] L. Chen, Q.-G. Huang, and K. Wang, J. Cosmol. Astropart. Phys. 02 (2019) 028.

[92] E. Aubourg et al., Phys. Rev. D **92,** 123516 (2015).

[93] A. G. Riess, S. Casertano, W. Yuan, J. B. Bowers, L. Macri, J. C. Zinn, and D. Scolnic, Astrophys. J. Lett. **908,** L6 (2021).

[94] D. Foreman-Mackey, D. W. Hogg, D. Lang, and J. Goodman, Publ. Astron. Soc. Pac. **125**, 306 (2013).

[95] W. J. Handley, M. P. Hobson, and A. N. Lasenby, Mon. Not. R. Astron. Soc. **450**, L61 (2015).

[96] A. Lewis, arXiv:1910.13970.

[97] R. E. Kass and A. E. Raftery, J. Am. Stat. Assoc. **90**, 773 (1995).

[98] T. Barreiro, E. J. Copeland, and N. J. Nunes, Phys. Rev. D **61**, 127301 (2000).

[99] A. R. Liddle and R. J. Scherrer, Phys. Rev. D **59**, 023509 (1998).